Results in Chemistry 3 (2021) 100116

Contents lists available at ScienceDirect

Results in Chemistry

journal homepage: www.elsevier.com/locate/rechem

Theoretical studies on triplet formations in nitrobenzoxadiazole (NBD) derivatives: The impact of donor group and heteroatom substitution

Chao Wang [a,b], Hui Juan Koh [a], Zhaochao Xu [b,*], Xiaogang Liu [a,*]

[a] Fluorescence Research Group, Singapore University of Technology and Design, 8 Somapah Road, Singapore 487372, Singapore
[b] CAS Key Laboratory of Separation Science for Analytical Chemistry, Dalian Institute of Chemical Physics, Chinese Academy of Sciences, 457 Zhongshan Road, Dalian 116023, China

ARTICLE INFO

Keywords:
Nitrobenzoxadiazole
TD-DFT
Spin-orbital coupling
Molecular engineering

ABSTRACT

Heavy-atom-free triplet photosensitizers (TPs) have attracted much interest due to the applications in triplet–triplet annihilation (TTA) and photodynamic therapy. Recently, several nitrobenzoxadiazole (NBD) derivatives have been reported to generate singlet oxygens. However, the mechanistic understanding of the intersystem crossing (ISC) process has not been studied, resulting in a lack of rational design strategies for creating effective TPs. Based on DFT and TD-DFT calculations, we found that the replacement of donor group (methylamino → methoxyl) and the heteroatom (oxadiazole → triazole) could induce a significant change in the nature of triplet excited states in comparison to that of the single excited states, and thus enable substantial spin-orbital couplings for efficient triplet conversions. We expect that modifying the electronic properties of the triplet excited states through donor/heteroatom substitution is a promising method for creating heavy-atom-free TPs in many chemical families of fluorophores.

1. Introduction

Organic fluorophores with readily accessible triplet excited states have been widely used in various applications, such as organic semiconductors [1], thermally activated delayed fluorescence (TADF) [2], phosphorescent bioimaging [3], room temperature phosphoresce (RTP) [4,5], triplet–triplet annihilation (TTA) for photon upconversion [6], and photodynamic therapy [7–9]. Among various triplet sensitizers, heavy-atom-free triplet photosensitizers (TPs) are highly attractive, owing to their low toxicity, low costs, excellent light absorbance, and long-lived triplet excited states [10]. Yet, rational design guidelines for creating effective heavy-atom-free TPs remains lacking.

Through structural modifications, conventional fluorophores are often adopted in the molecular engineering of heavy-atom-free TPs. For example, xanthone derivatives were reported to have a significant triplet formation yield (>0.5) [11,12]. Ketocoumarins possessed a high singlet oxygen generation yield of 0.28–0.48 [13]. Yoon and co-workers developed several efficient naphthalimide-based TPs by replacing oxygen with sulfur atoms [14]. The substitutions of the aromatic ring at the meso-position in BODIPY derivatives could activate the excited state charge separation [15,16] and enhance the spin-orbital charge-transfer intersystem crossing (SOCT-ISC) for high-performance TPs as well [9,17–19].

Besides, nitrobenzoxadiazole (NBD) derivatives were frequently used in various biological studies, owing to their high environmental sensitivity, excellent biocompatibility, small molecular size, and charge neutrality [20–22]. Santa and co-workers reported that the replacement of methylamino with methoxyl in NBD-based dyes could significantly quench the fluorescence with a considerable triplet formation yield of 0.21 in acetonitrile [23]. PM3-CAS/CI calculations suggested that minimizing the S_1-T_2 energy gap is key in populating triplet excited states [24]. Recently, Norris et al. reported that the methoxyl substituted isobenzofuran-based fluorophores showed potential in generating single oxygens, which is very different from the emissive behavior of methylamino substituted NBD analogues (Fig. 1a) [25].

However, the intersystem crossing (ISC) processes in isobenzofuran-based NBD derivatives have not been studied, as ISC is too fast for conventional experimental techniques to investigate. In this paper, we studied the impact of both donor and heteroatom substitutions on the photophysical properties and ISC process of these NBD derivatives using DFT and TD-DFT calculations. We further discussed the impact of heteroatom replacement in SCOTfluors [26] on

---

* Corresponding authors.
E-mail addresses: zcxu@dicp.ac.cn (Z. Xu), xiaogang_liu@sutd.edu.sg (X. Liu).

https://doi.org/10.1016/j.rechem.2021.100116
Received 11 December 2020; Accepted 5 February 2021

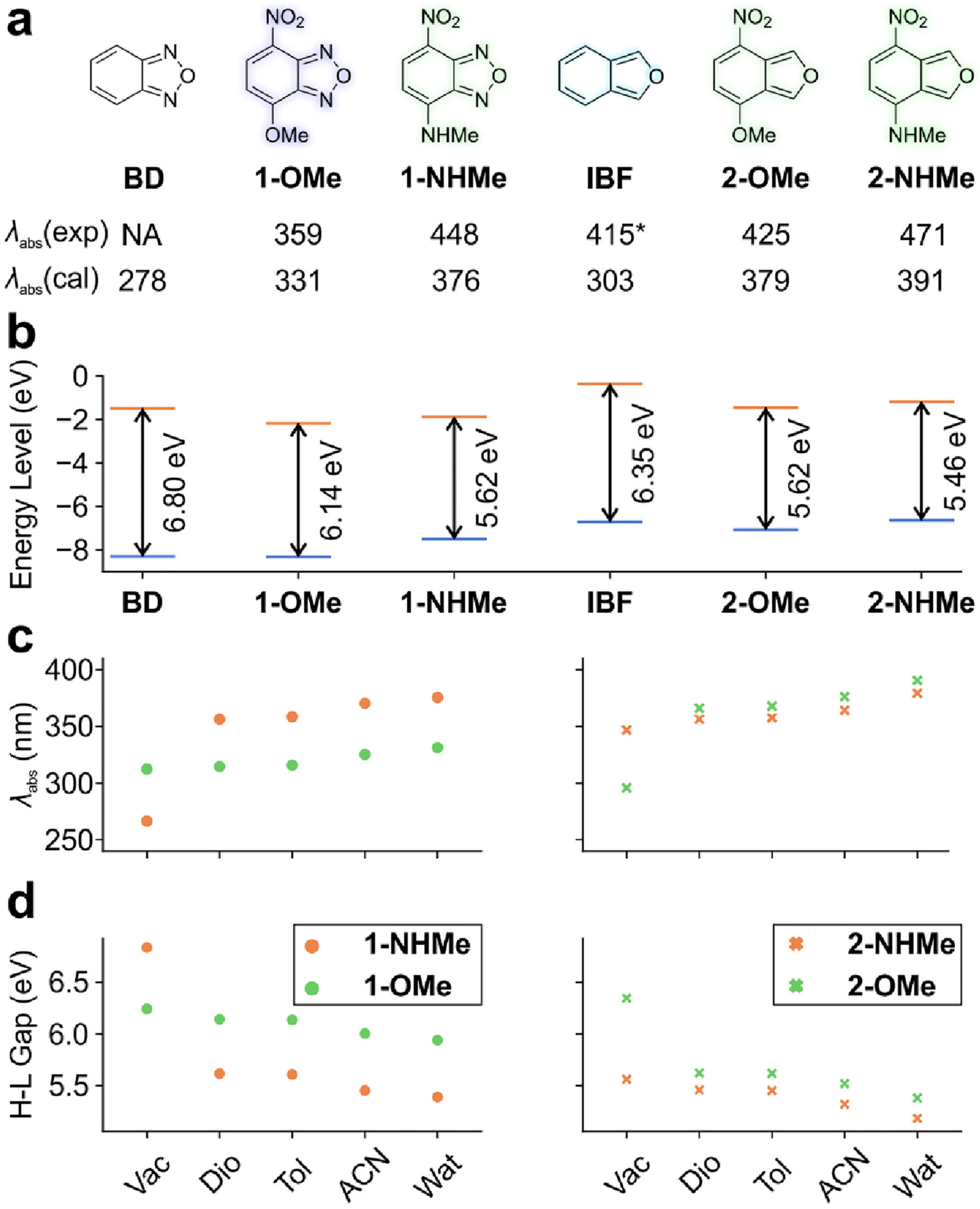

Fig. 1. (a) Chemical structures of benzoxadiazole and isobenzofuran scaffolds and fluorophores. (b) Energy levels of HOMO (Blue) and LUMO (Orange) of the Frank-Condon (FC) state, calculated at the M06-2X/def2-SVP level in dioxane. (c) Calculated λ_{abs} and (d) the corresponding HOMO-LUMO (H-L) gaps in various medium including vacuum (Vac), dioxane (Dio), toluene (Tol), acetonitrile (ACN), and water (Wat). *The spectroscopic data of **IBF** was adopted from its alkylated analogue measured in ether solvent, as data in dioxane is not available [33]. (For interpretation of the references to colour in this figure legend, the reader is referred to the web version of this article.)

the triplet formation ability. We showed that several NBD derivatives are promising candidates for high-performance TPs.

2. Computational details

The ground and excited state geometric optimizations and calculations of the corresponding absorption and emission properties were performed at the M06-2X/def2-SVP level using Gaussian 16 software [27]. Frequency calculations were utilized to ensure molecular geometries at the local minima on potential energy surfaces. The SMD solvent model was used in all calculations for including the solvation effect [28]. Natural transition orbitals (NTOs) [29] and charge transfer distance (d_{CT}) [30] were calculated through Multiwfn 3.4.0 [31]. The SOCs between S_1 and T_n were evaluated based on the S_1 geometry at the M06-2X/def2-SVP level using ORCA 4.1.1 [32].

3. Results and discussion

We first rationalized the impact of heteroatoms and donor substituents on the maximum UV–vis absorption (λ_{abs}) wavelengths of NBD derivatives (Fig. 1). Experimental data showed that isobenzofuran (**IBF**)-based fluorophores had redshifted λ_{abs} in comparison to benzoxadiazole (**BD**)-based analogues (i.e., with the same donor groups; Fig. 1a). Moreover, methylamino (NHMe) substitution led to more significant redshifts in λ_{abs} than the methoxyl (OMe) group does for both **BD** and **IBF**-based fluorophores. Quantum chemical calculations using M06-2X functional successfully reproduced these trends, although M06-2X underestimated λ_{abs}. These absolute deviations are mainly because M06-2X has a large fraction of Hartree–Fock (HF) exchange [15]. Compared to the DFT exchange, HF exchange can result in more bound valance electron density, which may overestimate the HOMO-LUMO energy gap as well as the excitation energies.

For long-range intramolecular charge transfer (ICT) excitations, the excitation energy can be roughly estimated through the following equation [34]:

$$E_{ICT} \approx IP_D - EA_A - 1/R \tag{1}$$

where IP_D is the ionization potential of the donor group, and EA_A is the electron affinity of the acceptor group. Due to the similar sizes of NBD-like fluorophores (similar R in Eq. (2)), the HOMO-LUMO gap is key to understand the change of λ_{abs} when the S_1 excitation is dominated by the HOMO-LUMO transition. We observed that the HOMO-LUMO gap of **IBF** (6.35 eV) is much smaller than **BD** (6.80 eV) (Fig. 1b). Such tendency remains when OMe and NHMe groups were substituted to **IBF** and **BD** scaffolds, respectively. In short, the replacement of nitrogen with carbon (**BD** → **IBF**) leads to a decrease in the HOMO-LUMO gap, which induces the redshift of λ_{abs}.

Meanwhile, the NHMe-substituted fluorophores showed higher HOMO energy levels compared with the OMe-substituted ones, thus yielding narrower HOMO-LUMO gaps. This is mainly because the NHMe group has a slightly stronger electron-donating ability than the OMe group. The narrower HOMO-LUMO gaps thus induce the redshift of λ_{abs} in NHMe-substituted fluorophores in comparison to OMe-substituted ones.

We then evaluated the impact of solvent polarity on λ_{abs} and HOMO-LUMO gaps (Fig. 1c, d). Generally, λ_{abs} and HOMO-LUMO gaps decrease with the increase in the solvent polarity. This trend is in good agreement with the experimental data as these fluorophores have positive solvatochromism [25]. Calculations also indicate that **1-NHMe** exhibited more sensitivity to the solvent polarity than **1-OMe** as the HOMO-LUMO reduces more rapidly. These calculations are fully consistent with experimental observations. For example, experimental measurements showed that the λ_{abs} of **1-NHMe** experienced a redshift of 36 nm from toluene to water, *c.f.* 13 nm for **1-OMe** [25].

In contrast, the HOMO-LUMO gap of **2-OMe** decreased more sharply than **2-NHMe** did as solvent polarity increases. Since the electron-donating ability of NHMe is slightly stronger than OMe, this reverse tendency suggests that the **IBF** core may greatly affect the solvatochromism in **2-OMe**. Indeed, experiments also showed that the λ_{abs} of both **2-OMe** and **2-NHMe** showed considerable redshifts by ~ 35 nm from toluene to water. In terms of the peak emission wavelengths (λ_{em}), the corresponding redshift in **2-OMe** (102 nm) is significantly larger than that in **2-NHMe** (53 nm) [25].

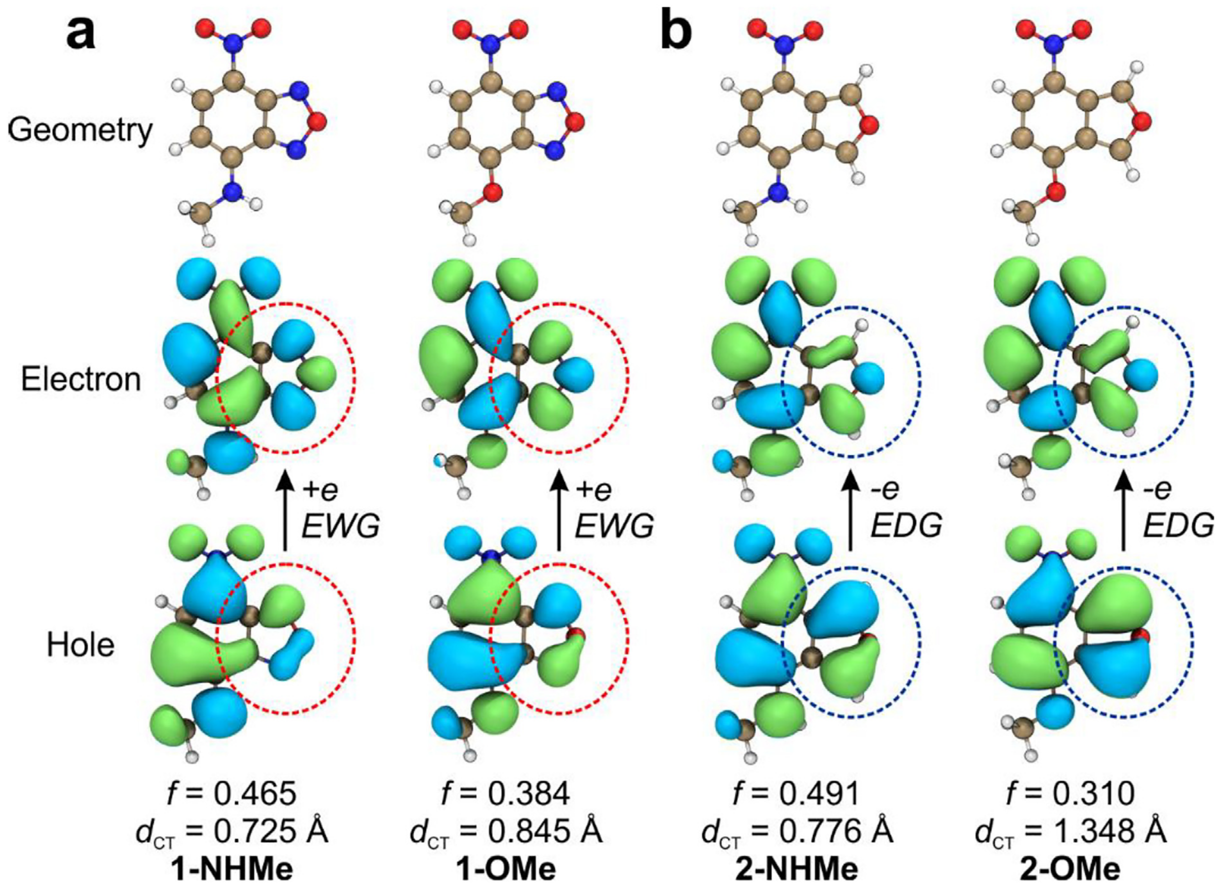

Fig. 2. S_1 electron and hole NTOs of the FC state of (a) **1-NHMe** and **1-OMe** and (b) **2-NHMe** and **2-OMe**, calculated at the M06-2X/def2-SVP level in dioxane. The oscillator strength (*f*) and charge transfer distance (d_{CT}) are labeled in the inset.

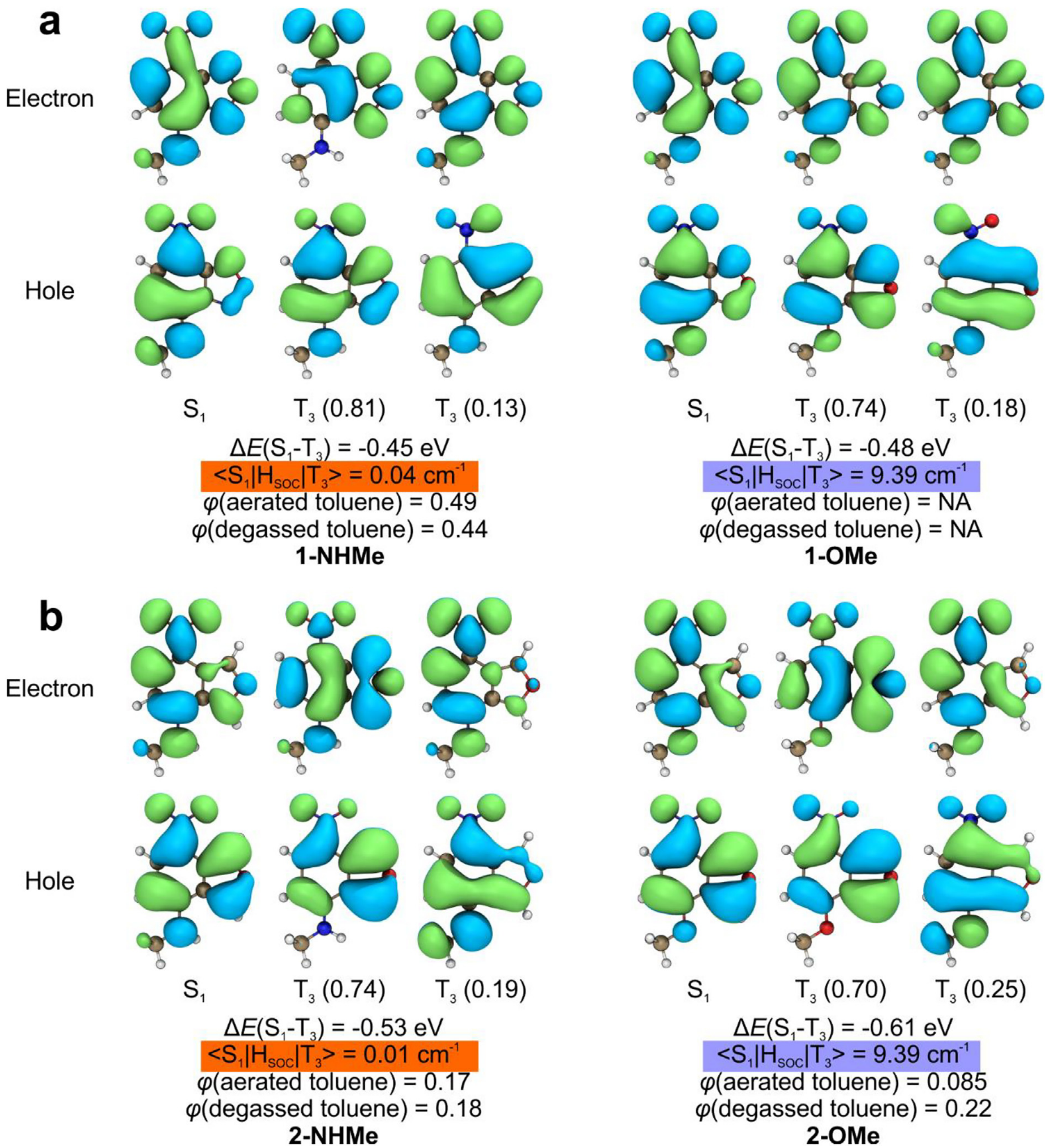

Fig. 3. Electron and hole NTOs for (a) **1-NHMe** and **1-OMe** and (b) **2-NHMe** and **2-OMe** calculated at the M06-2X/def2-SVP level based on the optimized S_1 geometry in water. The coefficients of NTOs, singlet–triplet differences, SOCs, and quantum yields in aerated and degassed toluene are labeled in the inset. We used water solvent as the linear-response formalism may significantly underestimate the solvent polarization.

To gain a deeper understanding on the different degrees of solvatochromism, we probed the nature of Frank-Condon (FC) states for assessing the impact of heteroatoms and donor groups on the solvatochromism using both natural transition orbitals (NTO) [29] and charge-transfer distance (d_{CT}) [30] analysis (Fig. 2). Our calculations suggest that **1-NHMe** (d_{CT} = 0.725 Å) and **1-OMe** (d_{CT} = 0.845 Å) experience a similar CT degree (Fig. 2a). We also observed that the furazan fragment functions as an electron-withdrawing group (EWG) as the electron density slightly accumulated on electron NTO in comparison to the hole NTO. As a result, the larger solvatochromism in **1-NHMe** than **1-OMe** is attributed to a stronger push–pull effect, which affords a more substantial reduction of the HOMO-LUMO gap as the solvent polarity increases (Fig. 1c).

Next, we investigated the nature of the FC states in **2-NHMe** and **2-OMe** (Fig. 2b). We noted that OMe substitution (d_{CT} = 1.348 Å) results in an enhanced charge transfer compared to the NHMe group (d_{CT} = 0.845 Å) in **IBF**-based fluorophores. Interestingly, the furan fragment served as an electron-donating group (EDG) as the electron density declined on the electron NTO compared to hole NTO. Our calculations underlined that the combination of **IBF** core with OMe substitution leads to an enhanced ICT transition, endowing **2-OMe** with substantial solvatochromism.

Inspired by these good agreements between quantum chemical calculations and experimental measurements, we next explored the molecular origins of the distinct quantum yields in these compounds. Experimental data suggested that the quantum yields of **1-NHMe**

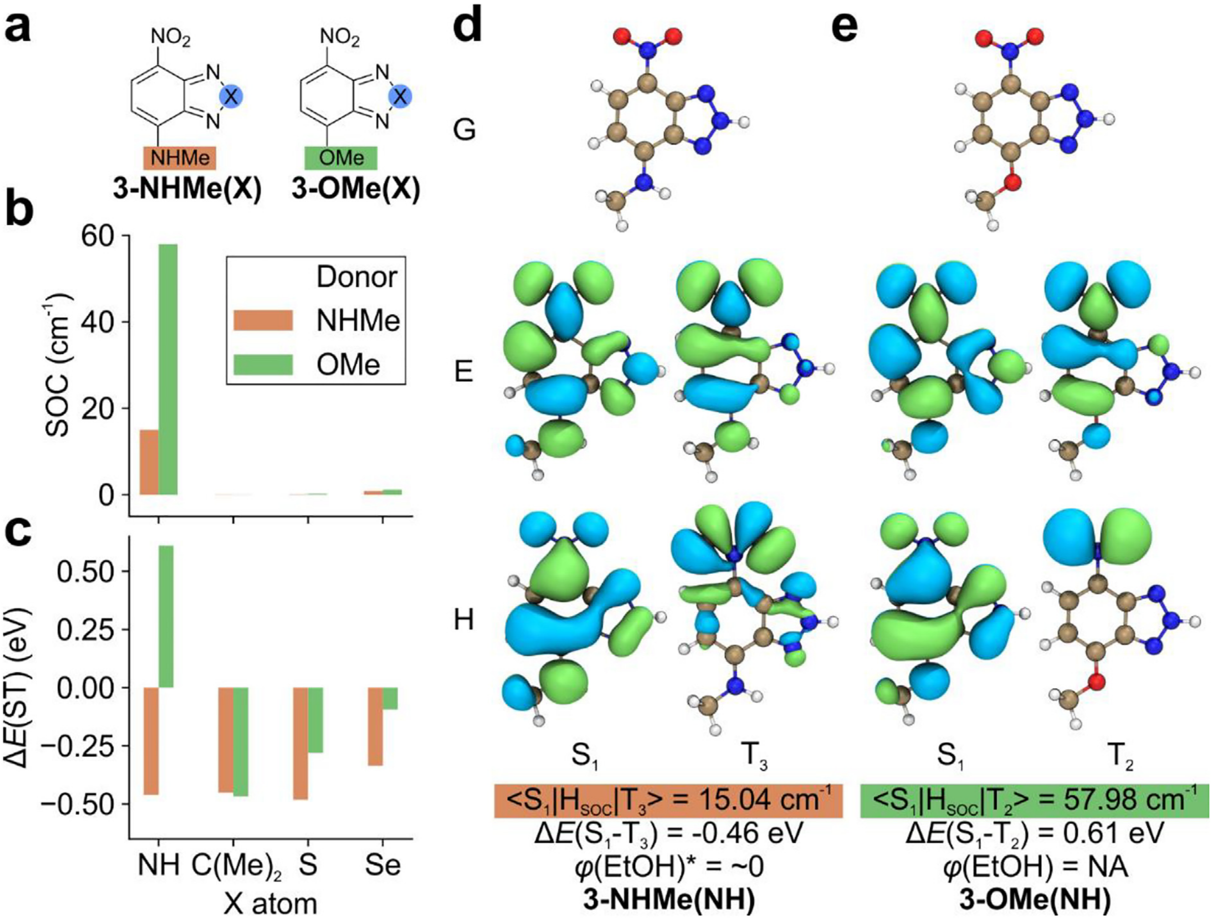

Fig. 4. (a) Chemical structures of SCOTfluoros. (b) SOC and (c) Δ*E*(ST) as a function of the heteroatom X. Molecular geometries, electron and hole NTOs for **3-NHMe(NH)** and **3-OMe(NH)** calculated at the M06-2X/def2-SVP level based on the optimized S_1 geometry in water. The SOC, singlet–triplet splitting, and quantum yield are labeled in the inset.

and **2-NHMe** showed little change when the solvent changed from aerated toluene to degassed toluene, while **2-OMe** exhibited a notable increase from 0.085 to 0.22 [25]. Such quantum yield change indicates the formation of triplet states in **2-OMe**.

According to the Fermi's Golden rule, the ISC rate constant (k_{ISC}) can be computed as follows [35,36]:

$$k_{ISC} = \frac{2\pi}{\hbar}\rho_{FC}|\langle S_1|H_{\mathrm{SOC}}|T_n\rangle|^2 \tag{2}$$

where $<S_1|H_{\mathrm{SOC}}|T_n>$ is the SOC matrix element between S_1 and T_n, ρ_{FC} denotes the Frank-Condon-weighted density of states. It is worth noting that ρ_{FC} will exponentially increase with the decrease in the gap between S_1 and T_n (ΔE_{ST}). We can learn from Eq. (1) that a small ΔE_{ST} along with a large SOC can prompt a rapid ISC process. Theoretical calculations thus play vital roles in designing TPs as it is likely the most efficient way of evaluating energy levels and probing the nature of excited states. Indeed, TD-DFT calculations were frequently utilized to understand the ISC process in terms of both energy levels and spin-orbital couplings (SOCs) [12,14,37–39].

Here we discussed the impact of heteroatoms and donor groups on the singlet–triplet splitting (Fig. 3). Generally, the replacement of NHMe with OMe lead to a small increase in $\Delta E(S_1\text{-}T_3)$ gaps (Fig. 3a). Such observations were also valid in **IBF**-based fluorophores (Fig. 3b). Meanwhile, the replacement of **BD** with **IBF** core also results in a slight increase in $\Delta E(S_1\text{-}T_3)$ by 0.08 eV in **2-NHMe** and by 0.13 eV in **2-OMe**. However, these marginal increases in $\Delta E(S_1\text{-}T_3)$ are not beneficial to the triplet conversion as the ISC process may become slow.

We also probed the natures of singlet and triplet excited states by comparing hole and electron NTOs. S_1 of **1-NHMe** and **1-OMe** exhibits a slight ICT character from the donor fragments (i.e., NHMe and OMe) to the fluorophore scaffolds (Fig. 3a). On the other hand, T_3 can be described by two pairs of NTOs. In **1-NHMe**, the major pair of NTO has an ICT transition from NHMe to the fluorophore scaffold, while the minor pair also shows an ICT nature from the furazan fragment to the fluorophore. For **1-OMe**, both NTO pairs indicated an ICT from the furazan fragment to the fluorophore. It was also observed that **1-OMe** showed increased fraction in the minor pair of NTOs with reduced fraction in the major pair than **1-NHMe** does. The El-Sayed rule [40] states that k_{ISC} becomes faster when the ISC process involves a change in the nature of excited states, namely, an enhanced SOC. As a result, **1-OMe** (9.39 cm^{-1}) had an improved SOC value than **1-NHMe** (0.04 cm^{-1}) as the nature of T_3 is much different from that of S_1. **1-OMe** was thus expected to have a much stronger triplet formation rate than **1-NHMe** does (by about 55,000 times if omitting other variables according to Eq. (1)) due to its enhanced SOC and similar energy level.

Indeed, experimental data from the Santa group showed that **1-NHMe** has negligible triplet formation yield, while this yield amounts to 0.21 for **1-OMe** in acetonitrile [23]. These data are fully consistent with our SOC calculations.

Similar observations were also found in **2-NHMe** and **2-OMe**, indicating that **2-OMe** would have strong triplet formation due to the enhanced SOCs. These computational results are also in good agreement with the increasing quantum yield of **2-OMe** from aerated to degassed toluene [25]. Overall, our calculations highlighted that the replacement of NHMe with OMe can induce substantial SOCs for triplet formation; the management of the nature of triplet excited states is key in prompting triplet conversions.

As our calculations successfully rationalized the triplet formations in **1-OMe** and **2-OMe**, we also studied the impact of heteroatoms on the triplet formations in SCOTfluoros (Fig. 4a) [41]. It can be seen that the –NH heteroatom replacement induces significant SOCs, namely, 15.04 cm^{-1} for NHMe donor (**3-NHMe(NH)**) and 57.98 cm^{-1} for OMe donor (**3-OMe(NH)**; Fig. 4b). Conversely, the $C(Me)_2$, S, and Se heteroatom replacements lead to relatively smaller SOCs around 2 cm^{-1}. It is interesting to note that the fluorescence of **3-NHMe (NH)** analogue is quenched in ethanol, while the rest SCOTfluoros are emissive (Fig. 4d) [41]. Apart from the state-crossing to an electron transfer state and hydrogen bonding interactions [26], the triplet formation may also contribute to the fluorescence quenching. In short, our calculation suggests that the –NH heteroatom replacement may enhance the SOC for fast triplet formations.

Finally, we rationalized the substantial SOCs in **3-NHMe(NH)** and **3-OMe(NH)** (Fig. 4d-e). Electron and hole NTOs suggested that S_1 of **3-NHMe(NH)** and **3-OMe(NH)** were described by a slight ICT nature from the donor fragment to the fluorophore (or π-π^* transitions), exhibiting a similar S_1 nature as the case of **BD** and **IBF**-based fluorophores. Interestingly, the triplet excited states responsible for the ISC process showed the n-π^* transition, which is markedly different from their π-π^* nature in S_1. The n-π^* transition is further enhanced from **3-NHMe(NH)** to **3-OMe(NH)**, resulting in an increase of the SOCs from 15.04 cm^{-1} to 57.98 cm^{-1}. These results suggest that the -OMe replacement is also effective in –NH substituted SCOTfluoros for facilitating triplet formations.

4. Conclusion

In this paper, we applied DFT and TD-DFT calculations to discuss the impact of the donor group and heteroatoms on the photophysical properties and triplet formations of NBD derivatives. We found that the replacement of oxadiazole with furan fragment in these fluorophores resulted in the redshift of λ_{abs}. Importantly, the replacement of NHMe with OMe group and the replacement of heteroatom from oxygen to nitrogen (oxadiazole → triazole) can induce significant SOCs for triplet conversions. The management of the distinct nature of triplet excited states in comparison to that of the singlet is key for achieving efficient triplet conversion in these NBD derivatives.

CRediT authorship contribution statement

Chao Wang: Conceptualization, Methodology, Writing - original draft, Writing - review & editing. **Hui Juan Koh:** Methodology. **Zhaochao Xu:** Writing - review & editing, Funding acquisition. **Xiaogang Liu:** Conceptualization, Writing - review & editing, Project administration, Funding acquisition.

Declaration of Competing Interest

The authors declare that they have no known competing financial interests or personal relationships that could have appeared to influence the work reported in this paper.

Acknowledgements

The authors thank the support from A*STAR under its Advanced Manufacturing and Engineering Program (A2083c0051), Dalian Institute of Chemical Physics (TMSR201601, DMTO201603), and the National Natural Science Foundation of China (21878286, 21908216). The authors are grateful for the super-computing resources of SUTD-MIT IDC and the National Supercomputing Centre (Singapore).

References

[1] A. Köhler, H. Bässler, Mater. Sci. Eng. R Rep. 66 (2009) 71–109.

[2] W. Chen, F. Song, Chin. Chem. Lett. 30 (2019) 1717–1730.

[3] Q. Zhao, C. Huang, F. Li, Chem. Soc. Rev. 40 (2011) 2508–2524.

[4] Z. An, C. Zheng, Y. Tao, R. Chen, H. Shi, T. Chen, Z. Wang, H. Li, R. Deng, X. Liu, W. Huang, Nat. Mater. 14 (2015) 685–690.

[5] G. Qu, Y. Zhang, X. Ma, Chin. Chem. Lett. 30 (2019) 1809–1814.

[6] T.N. Singh-Rachford, F.N. Castellano, Coord. Chem. Rev. 254 (2010) 2560–2573.

[7] D.W. Felsher, Nat. Rev. Cancer 3 (2003) 375–380.

[8] Y. Chen, L. Li, W. Chen, H. Chen, J. Yin, Chin. Chem. Lett. 30 (2019) 1353–1360.

[9] K. Chen, Y. Dong, X. Zhao, M. Imran, G. Tang, J. Zhao, Q. Liu, Front. Chem. 7 (2019) 821.

[10] J. Zhao, W. Wu, J. Sun, S. Guo, Chem. Soc. Rev. 42 (2013) 5323–5351.

[11] M. Jia, Z. Zhou, M. Lv, J. Chen, Chin. Chem. Lett. 29 (2018) 1486–1488.

[12] L.D. Elliott, S. Kayal, M.W. George, K. Booker-Milburn, J. Am. Chem. Soc. 142 (2020) 14947–14956.

[13] D. Huang, J. Sun, L. Ma, C. Zhang, J. Zhao, Photochem. Photobiol. Sci. 12 (2013) 872–882.

[14] V.N. Nguyen, S. Qi, S. Kim, N. Kwon, G. Kim, Y. Yim, S. Park, J. Yoon, J. Am. Chem. Soc. 141 (2019) 16243–16248.

[15] C. Wang, Q. Qiao, W. Chi, J. Chen, W. Liu, D. Tan, S. McKechnie, D. Lyu, X.F. Jiang, W. Zhou, N. Xu, Q. Zhang, Z. Xu, X. Liu, Angew. Chem., Int. Ed. 59 (2020) 10160–10172.

[16] W. Chi, J. Chen, W. Liu, C. Wang, Q. Qi, Q. Qiao, T.M. Tan, K. Xiong, X. Liu, K. Kang, Y.T. Chang, Z. Xu, X. Liu, J. Am. Chem. Soc. 142 (2020) 6777–6785.

[17] J.T. Buck, A.M. Boudreau, A. DeCarmine, R.W. Wilson, J. Hampsey, T. Mani, Chem 5 (2019) 138–155.

[18] Z. Wang, J. Zhao, Org. Lett. 19 (2017) 4492–4495.

[19] M. Liu, S. Ma, M. She, J. Chen, Z. Wang, P. Liu, S. Zhang, J. Li, Chin. Chem. Lett. 30 (2019) 1815–1824.

[20] X. Zhang, L. Yuan, J. Jiang, J. Hu, A. du Rietz, H. Cao, R. Zhang, X. Tian, F. Zhang, Y. Ma, Z. Zhang, K. Uvdal, Z. Hu, Anal. Chem. 92 (2020) 3613–3619.

[21] I. Ismail, Z.Y. Chen, L. Sun, X.R. Ji, H.S. Ye, X.Y. Kang, H.J. Huang, H.B. Song, S.G. Bolton, Z. Xi, M.D. Pluth, L. Yi, Chem. Sci. 11 (2020) 7823–7828.

[22] L. Yi, Z. Xi, Org. Biomol. Chem. 15 (2017) 3828–3839.

[23] S. Uchiyama, K. Takehira, S. Kohtani, K. Imai, R. Nakagaki, S. Tobita, T. Santa, Org. Biomol. Chem. 1 (2003) 1067–1072.

[24] S. Uchiyama, T. Santa, N. Okiyama, K. Azuma, K. Imai, J. Chem. Soc., Perkin Trans. 2 (2000) 1199–1207.

[25] S.R. Norris, C.C. Warner, B.J. Lampkin, P. Bouc, B. VanVeller, Org. Lett. 21 (2019) 3817–3821.

[26] Y. Gao, C. Wang, W. Chi, X. Liu, Chem. Asian J. 15 (2020) 4082–4086.

[27] M.J. Frisch, G.W. Trucks, H.B. Schlegel, G.E. Scuseria, M.A. Robb, J.R. Cheeseman, G. Scalmani, V. Barone, G.A. Petersson, H. Nakatsuji, X. Li, M. Caricato, A.V. Marenich, J. Bloino, B.G. Janesko, R. Gomperts, B. Mennucci, H.P. Hratchian, J.V. Ortiz, A.F. Izmaylov, J.L. Sonnenberg, Williams, F. Ding, F. Lipparini, F. Egidi, J. Goings, B. Peng, A. Petrone, T. Henderson, D. Ranasinghe, V.G. Zakrzewski, J. Gao, N. Rega, G. Zheng, W. Liang, M. Hada, M. Ehara, K. Toyota, R. Fukuda, J. Hasegawa, M. Ishida, T. Nakajima, Y. Honda, O. Kitao, H. Nakai, T. Vreven, K. Throssell, J.A. Montgomery Jr., J.E. Peralta, F. Ogliaro, M.J. Bearpark, J.J. Heyd, E.N. Brothers, K.N. Kudin, V.N. Staroverov, T.A. Keith, R. Kobayashi, J. Normand, K. Raghavachari, A.P. Rendell, J.C. Burant, S.S. Iyengar, J. Tomasi, M. Cossi, J.M. Millam, M. Klene, C. Adamo, R. Cammi, J.W. Ochterski, R.L. Martin, K. Morokuma, O. Farkas, J.B. Foresman, D.J. Fox, Gaussian 16, Wallingford, CT, 2016.

[28] A.V. Marenich, C.J. Cramer, D.G. Truhlar, J. Phys. Chem. B 113 (2009) 6378–6396.

[29] R.L. Martin, J. Chem. Phys. 118 (2003) 4775–4777.

[30] C.A. Guido, P. Cortona, B. Mennucci, C. Adamo, J. Chem. Theory Comput. 9 (2013) 3118–3126.

[31] T. Lu, F. Chen, J. Comput. Chem. 33 (2012) 580–592.

[32] F. Neese, WIREs Comput. Mol. Sci. 8 (2018) e1327.

[33] R. Adams, M.H. Gold, J. Am. Chem. Soc. 62 (1940) 2038–2042.

[34] J. Autschbach, Chemphyschem 10 (2009) 1757–1760.

[35] V. Lawetz, G. Orlandi, W. Siebrand, J. Chem. Phys. 56 (1972) 4058–4072.

[36] G.W. Robinson, R.P. Frosch, J. Chem. Phys. 38 (1963) 1187–1203.

[37] C. Wang, C. Deng, D. Wang, Q.S. Zhang, J. Phys. Chem. C 122 (2018) 7816–7823.

[38] C. Wang, Q. Zhang, J. Phys. Chem. C 123 (2018) 4407–4416.

[39] P.K. Samanta, D. Kim, V. Coropceanu, J.L. Bredas, J. Am. Chem. Soc. 139 (2017) 4042–4051.

[40] M.A. El-Sayed, J. Chem. Phys. 38 (1963) 2834–2838.

[41] S. Benson, A. Fernandez, N.D. Barth, F. de Moliner, M.H. Horrocks, C.S. Herrington, J.L. Abad, A. Delgado, L. Kelly, Z. Chang, Y. Feng, M. Nishiura, Y. Hori, K. Kikuchi, M. Vendrell, Angew. Chem., Int. Ed. 58 (2019) 6911–6915.